



Magnetic and mechanical properties in FeXSiB (X=Cu, Zr, Co) amorphous alloys

P. Kwapuliński*, J. Rasek, Z. Stokłosa, G. Badura, B. Kostrubiec,
G. Haneczok

Institute of Materials Science, University of Silesia,
ul. Bankowa 12, 40-007 Katowice, Poland

* Corresponding author: E-mail address: pkwapuli@us.edu.pl

Received 30.01.2008; published in revised form 01.05.2008

ABSTRACT

Purpose: The idea of the paper is to study the influence of different alloying additions (Cu, Zr, Nb) on structural relaxation, crystallization, and improvement of soft magnetic properties in amorphous alloys of the type FeXSiB obtained by melt spinning technique.

Design/methodology/approach: Magnetic and electric characteristics of the as quenched and successively annealed samples were determined at room temperature. Experiments were carried out by applying magnetic permeability measurements (Maxwell-Wien bridge), magnetic after effects, resistivity (four points probe), magnetostriction coefficient (infrared optical sensor) and magnetization (magnetic balance and fluxmeter).

Findings: It was shown that soft magnetic properties of the examined alloys can be optimized by applying 1-h annealing at a specific temperature. The process of the improvement of soft magnetic properties is found to be diffusion controlled. The Arrhenius parameters of this process were determined by applying magnetic measurements.

Research limitations/implications: The obtained results are a part of a broad area of examinations devoted to establishing of the influence of different alloying additions and thermal annealing on soft magnetic properties of amorphous alloys obtained by melt spinning technique.

Practical implications: The examined alloys belong to a modern group of soft magnetic materials, which can be used as core transformers, magnetic sensors, shields of magnetic, electric and electromagnetic fields etc. The obtained results may be used for preparing soft magnetic ribbons for specific applications.

Originality/value: The originality of the paper lies in examination of the improvement of soft magnetic properties effect as a diffusion-controlled process. The influence of different alloying additions on the course of this process is well established.

Keywords: Amorphous materials; Nanocrystalline alloys; Soft magnetic properties; Structural relaxation; Crystallization

MATERIALS

1. Introduction

The past decade has seen the rapid development of different kinds of metallic glasses [1-6]. In this group especially important are amorphous soft magnetic alloys based on iron obtained by

melt spinning technique usually in a form of thin ribbons. Indeed, these alloys in relation to the conventional silicon steel are much cheaper and exhibit better magnetic as well as electrical and mechanical properties. It is obvious that the melt-spun ribbons are not in thermodynamic equilibrium and show relatively high content of the so-called free volume (microvoids) frozen during

fast cooling from liquid phase. This free volume content on one hand accelerates diffusion processes (structural relaxation (SR), improvement of magnetic properties, crystallization) and on the other hand strongly influences different physical properties.

The structural relaxation taking place at temperatures below the crystallization temperature has usually two components – irreversible one (Topological Short Range Ordering (TSRO)) and reversible one (Chemical Short Range Ordering (CSRO)). The TSRO process is due to redistribution and annealing out of microvoids, which is similar to annealing out of supersaturated vacancies in crystalline metals. The CSRO process is connected with atomic ordering of a given kind of atoms and is similar to atomic ordering in crystalline metals. The structural relaxation can be examined by applying different experimental techniques like magnetic permeability relaxation $\mu = \mu(t)$, resistivity ρ , viscosity coefficient η and positron annihilation. In any technique according to [7] the intensity of structural relaxation is proportional to free volume (microvoids) content.

2. Material and experimental procedure

The examinations were carried out for amorphous alloys $\text{Fe}_{78}\text{Si}_{13}\text{B}_9$, $\text{Fe}_{77}\text{Cu}_1\text{Si}_{13}\text{B}_9$, $\text{Fe}_{76}\text{Zr}_2\text{Si}_{13}\text{B}_9$ and $\text{Fe}_{74}\text{Cu}_1\text{Co}_1\text{Zr}_2\text{Si}_{13}\text{B}_9$ obtained in the form of strips (thickness and width of about 20 μm and 10 mm, respectively) by melt spinning technique. As quenched samples were annealed in vacuum at temperatures ranging from 300 to 900 K for different times i.e. isothermal and isochronal annealing with different step heating rate was used. The phase analysis for annealed samples was carried out by X-ray diffraction method (Philips X-Pert diffractometer) and high-resolution electron microscopy (JEM 3010). Magnetic permeability at weak fields (0.5 A/m) was measured by applying Maxwell-Wien bridge working at frequency of about 1 kHz.

The change of microvoids content in annealed samples was determined by applying two methods: i) magnetic permeability relaxation i.e. by measuring $\Delta\mu/\mu = (\mu(t_1) - \mu(t_2))/\mu(t_1)$ at room temperature (where $t_1=30\text{s}$ and $t_2=1800\text{s}$ are times after demagnetization) and ii) measurements of resistivity ρ at liquid nitrogen temperature using a four points probe with nanovoltmeter.

Diffusion parameters and reaction order for microvoids diffusion were determined for amorphous alloy kept at liquid nitrogen directly after production. The data analysis was based on the kinetics rate equation of the form:

$$\frac{dc}{dt} = K \cdot c^\gamma \quad (1)$$

where c is the microvoids content, γ is the reaction order. The reaction rate K depends on temperature T and is given by the Arrhenius relation:

$$K = K_0 \cdot \exp\left(\frac{E}{k_B T}\right) \quad (2)$$

where E is the activation energy, K_0 is the so-called preexponential factor and k_B is the Boltzmann constant.

Magnetic characteristics of the examined material were determined by applying digital fluxmeter, coercivimeter (permalloy probe) and magnetic balance. Magnetostriction coefficient was measured by making use of Joule and Villari effects [8,9]. The crystallization was examined by applying resistivity measurements with different heating rates (0.5 – 10 K/min) and the data analysis based on the Kissinger method [10].

3. Results and discussion

The structural relaxation in amorphous alloys based on iron plays an important role causing time instability of magnetic parameters. Fig. 1 shows isochronous curves of structural relaxation intensity determined via magnetic relaxation versus temperature T_a of the 1-hour annealing at elevated temperatures. The intensity $\Delta\mu/\mu$ being proportional to microvoids content depends on the kind of alloying addition. And so, Cu atoms in FeXSIB alloy cause an increase of the observed instabilities. In contrast to this Zr atoms cause a decrease of free volume content and what follows a reduction of time instabilities. Such a behaviour can be explain based on the model of metals melting which predicts that free volume content frozen into material decreases with increasing the melting point of alloying addition [11,12].

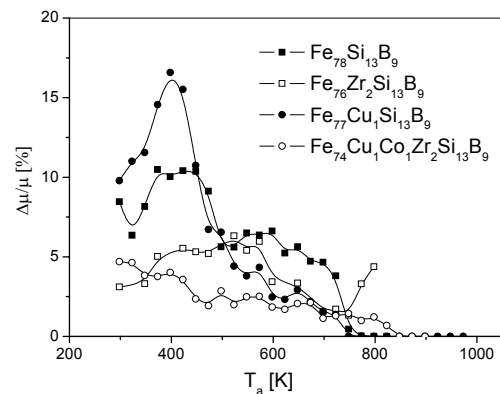


Fig. 1. Magnetic after effects determined at room temperature for samples annealed for 1-h at temperature T_a versus T_a

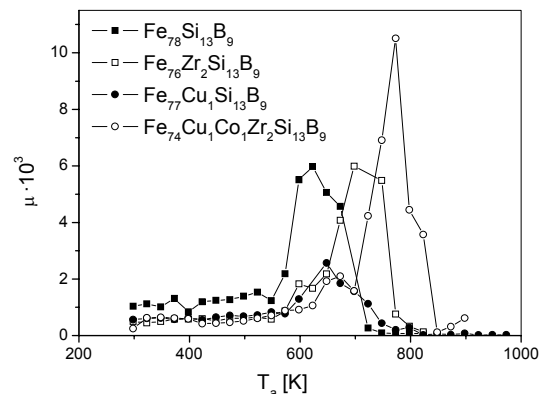


Fig. 2. Relative initial magnetic permeability determined at room temperature for samples annealed for 1-h at temperature T_a versus T_a

The analysis of the isothermal resistivity curves measured at 353 K and 363 K shows that kinetics of coagulation of microvoids in the $\text{Fe}_{78}\text{Si}_{13}\text{B}_9$ alloy for initial times can be described as reaction of the second order i.e. with $\gamma = 2.3$ and $\gamma = 2.1$, respectively. Parameters of the Arrhenius relation for irreversible component of structural relaxation were found to be $E_{\text{rel}}=1.03$ eV, $K_{\text{rel}}=3 \cdot 10^{14} \text{ s}^{-1}$. It is proper to add that similar values of γ were reported in [13] where measurements of viscosity coefficient were used.

Fig. 2 shows isochronous curves of initial magnetic permeability determined for samples annealed at temperatures T_a for 1-h. It can be seen that in all cases the curve $\mu(T_a)$ shows a maximum positioned at temperature being per definition the 1-h optimization annealing temperature T_{op} . According to Fig.2 the permeability values at maximum $\mu(T_{op})$ and the temperature T_{op} strongly depend on alloying addition.

The process of improvement of soft magnetic properties, demonstrated in Fig. 2, is a diffusion controlled process. Its nature was examined in detail using permeability measurements for samples isothermally annealed. In this kind of experiments magnetic permeability μ is measured at room temperature for samples successively annealed for a given time t at constant elevated temperature. The curve $\mu(t)$ shows a maximum for a characteristic annealing time τ . It was stated that τ depends on temperature and for higher temperatures the observed maximum shifts into shorter annealing times. Fig. 3 shows the Arrhenius plot i.e. $\ln(\tau)$ versus $1/T$ for the $\text{Fe}_{78}\text{Si}_{13}\text{B}_9$ alloy. Parameters of the Arrhenius relation calculated from the data of Fig. 3 are found to be $E = (1.4 \pm 0.2)$ eV, $\tau_0 = 7 \cdot 10^{9 \pm 2}$ s. For the $\text{Fe}_{77}\text{Cu}_1\text{Si}_{13}\text{B}_9$ and $\text{Fe}_{74}\text{Cu}_1\text{Co}_1\text{Zr}_2\text{Si}_{13}\text{B}_9$ alloys the corresponding values are: $E = (1.3 \pm 0.2)$ eV, $\tau_0 = 4 \cdot 10^{8 \pm 3}$ s, $E = (2.3 \pm 0.2)$ eV, $\tau_0 = 3 \cdot 10^{12 \pm 2}$ s, respectively.

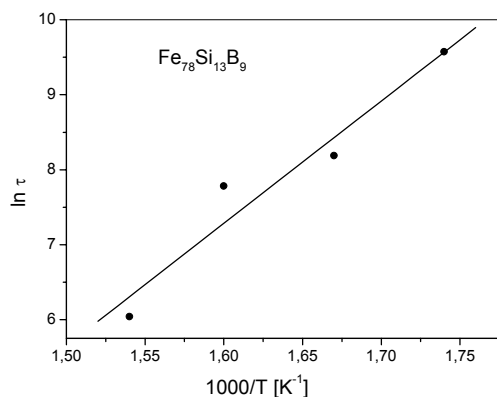


Fig. 3. Arrhenius plot $\ln(\tau)$ versus $1/T$ for the $\text{Fe}_{78}\text{Si}_{13}\text{B}_9$ alloy

Fig. 4 shows magnetostriction coefficient $\lambda_{||S}$ measured in parallel to saturation magnetic field direction $\lambda_{||S}$ versus 1-h annealing temperature T_a . Comparing the data of Figs. 2 and 4 one can conclude that samples with higher permeability show lower values of magnetostriction.

Fig. 5 shows an example of isochronous curves of the so-called fracture coefficient ε (defined as the ratio of sample thickness and the banding radius for which formation of fracture cracks were observed [14,15]) versus 1-h annealing temperature T_a .

Fig. 6 shows isochronous resistivity curves obtained with heating rate 0.5 K/min for samples of all examined alloys in the as quenched state. Similar measurements carried out with different heating rates (0.5 – 10 K/min) allows determining the overall activation energies for crystallization based on the shift of the homological points ($dp/dT=0$) with the heating rate. The obtained results are shown in Table 1, where the other characteristic quantities determined in this paper for different amorphous alloys are listed.

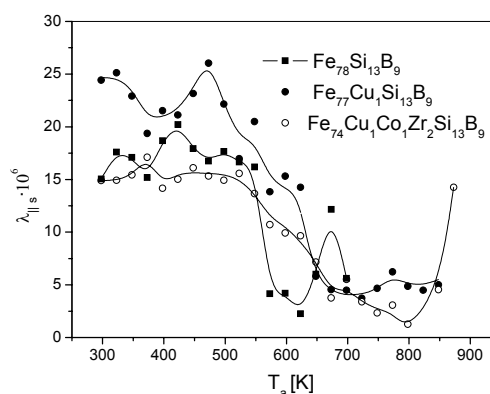


Fig. 4. Magnetostriction coefficient determined at room temperature measured parallel to magnetic field for samples annealed for 1-h at temperature T_a versus T_a

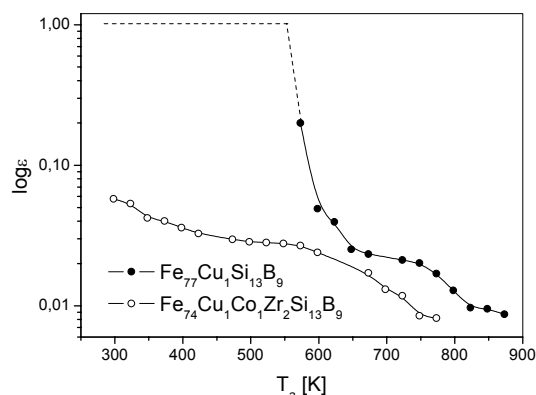


Fig. 5. Isochronous curves of the fracture coefficient ε determined for samples annealed for 1-h at temperature T_a versus T_a . Dashed line represents the data for the $\text{Fe}_{77}\text{Cu}_1\text{Si}_{13}\text{B}_9$ alloy annealed at $T_a < 550$ K for which the brittleness was unmeasurable small

The obtained results (X-ray diffraction analysis and high resolution electron microscopy observations) allows concluding that in the so-called primary crystallization formation of a nanocrystalline phase $\alpha\text{Fe}(\text{Si})$ is observed. At higher temperatures, in the secondary crystallization, borides Fe_2B and Fe_3B are formed. As it was already mentioned in amorphous alloys obtained by melt spinning technique microvoids frozen into materials affect kinetics of all thermally activated processes including crystallization.

Indeed, comparing the temperature of the primary crystallization (see Table 1) one can notice that for the $\text{Fe}_{77}\text{Cu}_1\text{Si}_{13}\text{B}_9$ alloy, for which the intensity of the structural relaxation ($\Delta\mu/\mu$) is the highest (see Fig. 1), the value of T_{x1} (682 K) is the lowest. The highest crystallization temperature is observed for the $\text{Fe}_{76}\text{Zr}_2\text{Si}_{13}\text{B}_9$ alloy for which $\Delta\mu/\mu$ is the lowest. Such a correlation can be explained basing on the model of metals melting. According to this model the content of frozen microvoids depends on the alloying addition and for Cu is the highest since the melting points for copper is the lowest (1357 K) in the examined group of alloying additions. The melting point for Zr is 2132 K which causes that the microvoids content for the $\text{Fe}_{76}\text{Zr}_2\text{Si}_{13}\text{B}_9$ alloy is the smallest. The observed correlation means that microvoids in amorphous alloys play similar role to supersaturated vacancies in crystalline alloys i.e. cause an acceleration of diffusion processes.

Table 1.

Optimisation of soft magnetic properties temperature T_{op} , temperatures of first and second stage of crystallisation T_{x1} , T_{x2} (for heating rate 0.5 K/min), the Curie temperature T_c , the activation energy of the first stage of crystallisation E_{k1} , electrical resistivity ρ , temperature coefficient of resistivity and Hall constant R_H at room temperature for investigated alloy in the as quenched state

Material	T_{op} [K]	T_{x1} [K]	T_{x2} [K]	T_c [K]	E_{k1} [eV]	ρ [10^{-8} Ω m]	α [10^{-4} /K]	R_H [n Ω m/T]
Fe ₇₈ Si ₁₃ B ₉	625	702	747	650	2.5±0.2	134	1.45	42
Fe ₇₆ Zr ₂ Si ₁₃ B ₉	700	795	—	640	2.6±0.2	170	0.63	57
Fe ₇₇ Cu ₁ Si ₁₃ B ₉	650	682	759	703	3.5 ± 0.4	161	1.54	60
Fe ₇₄ Cu ₁ Co ₁ Zr ₂ Si ₁₃ B ₉	773	738	867	633	4.5 ± 0.2	185	1.33	53

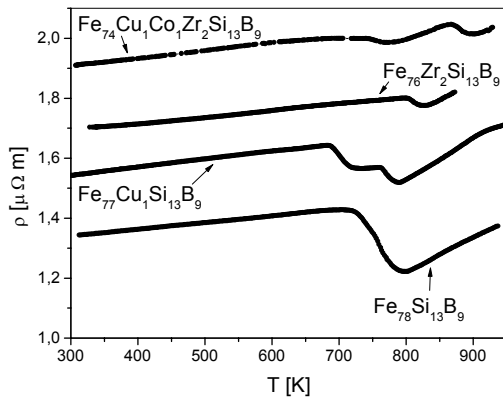


Fig. 6. Isochronous (in situ) resistivity curves obtained with heating rate 0.5 K/min

Let notice that for the amorphous alloys Fe₇₈Si₁₃B₉ and Fe₇₇Cu₁Si₁₃B₉ for which the content of microvoids in the as quenched state is relatively high the brittleness is relatively small (see Fig. 5). For the Fe₇₄Cu₁Co₁Zr₂Si₁₃B₉ alloy high value of brittleness is due to a low content of microvoids.

4. Conclusions

The main conclusions of the present paper can be summarized as follows:

1. Intensity of the structural relaxation in FeXSiB amorphous alloys strongly depends on chemical composition of the examined alloy and its time variation for initial times can be described by kinetics equation with the reaction order of 2.
2. The observed changes of structural relaxation intensity can be explain basing on the model of metals melting by taking into account the correlation between the melting point of alloying addition and the content of frozen microvoids in amorphous alloys.
3. Processes of the improvements of soft magnetic properties in FeXSiB amorphous alloys are diffusion controlled processes with activation energy of the order of 1 eV.

References

- [1] L.A. Dobrzański, M. Drak, B. Ziębowicz, Materials with specific magnetic properties, Journal of Achievements in Materials and Manufacturing Engineering 17 (2006) 37-40.

- [2] G. Badura, J. Rasek, Z. Stokłosa, P. Kwapiński, G. Haneczok, J. Lelaćko, L. Pająk, Soft magnetic properties enhancement effect and crystallization processes in Fe_{78-x}Nb_xSi₁₃B₉ amorphous alloys, Journal of Alloys and Compounds 436 (2007) 43-50.
- [3] S. Lesz, R. Nowosielski, A. Zajdel, B. Kostrubiec, Z. Stokłosa, Structure and magnetic properties of the amorphous Co₈₀Si₉B₁₁ alloy, Journal of Achievements in Materials and Manufacturing Engineering 18 (2006) 155-158.
- [4] D. Szewieczek, T. Raszka, J. Olszewski, Optimisation the magnetic properties of the (Fe_{1-x}Co_x)_{73.5}Cu₁Nb₃Si_{13.5}B₉ (X=10;30;40) alloys, Journal of Achievements in Materials and Manufacturing Engineering 20 (2007) 31-36.
- [5] S. Lesz, R. Nowosielski, B. Kostrubiec, Z. Stokłosa. Crystallisation kinetics and magnetic properties of a Co-based amorphous alloys, Journal of Achievements in Materials and Manufacturing Engineering 16 (2006) 35-39.
- [6] S. Lesz, R. Nowosielski, A. Zajdel, B. Kostrubiec, Z. Stokłosa, Investigation of crystallization behaviour of Co₈₀Si₉B₁₁ amorphous alloys, Archives of Materials Science and Engineering 28/2 (2007) 91-97.
- [7] R. Grössinger, R. Sato Turtelli, Amorphous and nanocrystalline alloys, IEEE Transactions on Magnetics 30 (1994) 455-460.
- [8] G. Vlasák, Z. Kaczowski, P. Duhaj, Magnetostriction of the Fe_{73.5}Cu₁Ta₂Nb₁Si_{13.5}B₉ alloy, Journal of Magnetism and Magnetic Materials 215-216 (2000) 476-478.
- [9] G. Vlasák, C. F. Conde, D. Jacičkovič, T. Svec, Magnetostriction measurements of (Fe-Co)-Mo-Cu-B alloys with varying atomic Fe/Co ratio, Materials Science and Engineering A 449-451 (2007) 464-467.
- [10] E. Illekova, J. Matko, P. Duhaj, F. A. Kunhast, The complex characteristics of crystallization of the Fe₇₅Si₁₅B₁₀ glassy ribbon, Journal of Materials Science 32 (1997) 4645-4654.
- [11] T. Górecki, M. Kostrzewa, Debye temperature for liquid metals and the vacancy model of melting, Acustica 77 (1993) 293-296.
- [12] T. Górecki, Cz. Górecki, K. Książek, S. Wacke, Effective vacancy formation energy and the solute - vacancy binding energy in binary Cu - based alloys Visnyk of the Lviv University, Series Khimichna 48 (2007) 88-94.
- [13] A. Van den Beukel, Structural relaxation in metallic glasses, Trends in non-crystalline solids, World Scientific Publishing Co., Singapore 1992.
- [14] H.Chiriac, C.Hison, Mechanical behavior of nanocrystalline Fe-Hf-B ribbons, Journal of Magnetism and Magnetic Materials 254-255 (2003) 475-476.
- [15] D. Szewieczek, J. Tyrlik-Held, S. Lesz, Structure and mechanical properties of amorphous Fe₈₄Nb₇B₉ alloy during crystallisation, Journal of Achievements in Materials and Manufacturing Engineering 24/2 (2007) 87-90.